Available online at www.sciencedirect.com
ScienceDirect
Polymer 48 (2007) 4900–4905
polymer
www.elsevier.com/locate/polymer

Study of the molecular weight dependence of glass transition temperature for amorphous poly(L-lactide) by molecular dynamics simulation

Jian Zhang, Yu Liang, Jizhong Yan, Jianzhong Lou*

Department of Mechanical and Chemical Engineering, North Carolina A&T State University, 1601 E. Market Street, Greensboro, NC 27411, USA

Received 4 May 2007; received in revised form 13 June 2007; accepted 16 June 2007
Available online 21 June 2007

Abstract

Molecular dynamics simulation has been used to investigate the molecular weight dependence of glass transition temperature for amorphous poly(L-lactide). Amorphous PLLA systems were created using molecular modeling and NPT ensemble MD simulations were carried out using the modified OPLS-AA force field. The fractal dimension of the PLA systems was 1.62. The molecular weight dependence of glass transition temperature, self-diffusion coefficient and shear viscosity were studied and the good agreement between the simulation results and experiments was obtained.
Published by Elsevier Ltd.

Keywords: Molecular dynamics simulation; Poly(L-lactide); Glass transition temperature

1. Introduction

The disposal problem due to nondegradable petroleum-based plastics has raised the demand for biodegradable polymers [1]. Poly(lactide) (PLA) is a biodegradable aliphatic polyester derived from 100% renewable resources, such as corn and sugar beets. Moreover, it has unique physical properties that make it useful in diverse applications including paper coating, fibers, films, and packaging [2]. Currently, PLA is primarily used for medical applications such as drug delivery devices, absorbable sutures, and as a material for medical implants and other related applications [3–13]. PLA, functionalized PLA and PLA block copolymers can be prepared by direct condensation or by the ring-opening polymerization [14–17]. The stereochemical microstructure of polymers can be controlled by the monomer composition in the feed or by the stereochemical preference of the initiating/catalytic system [18–20]. Phase transition behavior, morphology, miscibility and other physical properties of PLA-based nano-scale structures are widely studied recently [21–26]. All these nano-scale research and applications make the fundamental understanding of the PLA-based material at the molecular level a necessity.

Glass transition temperature T_g is of great importance concerning drug release, stability of the drug formulation and mechanical properties [27–30]. But current theories only can describe some aspects of glass transition phenomena correctly. There is no unified description that puts all the phenomena into one coherent framework. Experimentally, it was found that the main effect of varying degree of polymerization N is a shift of the glass transition temperature, which is a sensitive control parameter to check theories [32–33].

Molecular dynamics simulation has been used extensively in the study of different aspects of polymer structures and properties [34–38]. Recently, the resistance of PLA to hydrolysis based on the PLLA and PDLA blends and compatibility of PLLA and PVA blends were studied by molecular modeling simulations [28–29]. A new PLA force field developed by O'Brien using quantum mechanic calculations demonstrated quantitative improvement in performance compared to existing models [30]. Several approaches to determine the glass transition of polymers by computer simulations are reported. One common approach is to determine the kink in a graph

* Corresponding author. Tel.: +1 336 334 7620; fax: +1 336 334 7417.
E-mail address: lou@ncat.edu (J. Lou).

0032-3861/$ - see front matter Published by Elsevier Ltd.
doi:10.1016/j.polymer.2007.06.030

of the specific volume versus temperature originating from the change of the thermal expansion coefficient at T_g when passing from a glassy to a rubbery system [27]. Other approaches also use the increase of potential energy at T_g [39–41] or the temperature dependence of the mean-square displacement of polymer chains below and above T_g [27]. However, this simulation approach has not been used to calculate T_g for PLA.

The MD studies described in this work used the Groningen Machine for Chemical Simulation (GROMACS, version 3.3) software package [31]. The GROMACS software employs a Message Passing Interface (MPI) parallelization method, which enables it to be used on cluster-type supercomputers. This algorithm couples a simple one dimensional domain decomposition method with a cyclic calculation procedure. Although it was developed for biological molecules with complex bonded interactions, GROMACS is still suitable for MD simulations of nonbiological polymer systems because of its efficient calculation of nonbonded interactions. Its advanced algorithm and optimized coding also make it the fastest MD simulation package available [42–43].

In this paper, the usability of the new PLA force field developed by O'Brien [30] was examined by glass transition temperature determination using molecular dynamics simulation. The fractal dimension was calculated. Furthermore, the molecular weight dependence of glass transition temperature, self-diffusion coefficient and shear viscosity were studied. Our computational findings are supported by experiments and theories and provide insight into glass transition behavior of polymers.

2. Simulation details

2.1. Molecular modeling

The system potential energy was calculated using the GROMACS implementation of the modified OPLS-AA force field (Eq. (1)) [44]. The force field parameters were obtained from the new PLA force field developed by O'Brien [30].

$$E_{\mathrm{PE}} = \sum_{\text{bonds}} k_r (r - r_0)^2 + \sum_{\text{angles}} k_\theta (\theta - \theta_0)^2 + \sum_{\text{impropers}} k_\xi (\xi - \xi_0)^2 + \sum_{n=0}^{5} C_n (\cos(\psi))^n + \sum_i \sum_{j>i} f_{ij} \left\{ \frac{q_i q_j e^2}{r_{ij}} + 4\varepsilon_{ij} \left[\left(\frac{\sigma_{ij}}{r_{ij}} \right)^{12} - \left(\frac{\sigma_{ij}}{r_{ij}} \right)^{6} \right] \right\} \quad (1)$$

The nontorsional bonded interactions are modeled by first three harmonic terms for bond stretching, angle bending, and out of plane deformations for planar groups. The force constants for intramolecular deformations (k_r, k_θ, k_ξ) define the magnitude of the energy required to move the internal coordinates (r, θ, ξ) away from their unstrained default values (r_0, θ_0, ξ_0). The proper torsions are defined in terms of the specific dihedral angle (Ψ) and Ryckaert–Bellemans potential parameter C_n, where $n = 0, 1, \ldots 5$. The nonbonded interactions are modeled by Coulombic and 6-12 Lennard–Jones terms, where r_{ij} is the distance of two sites, q is the partial atomic charge, and σ_{ij} and ε_{ij} are the Lennard-Jones parameters. The scaling factor f_{ij} is 1.0 for all nonbonded interactions except for the 1,4-intramolecular interactions.

The amorphous PLA box containing 32 PLA chains were generated using Materials Studio 4.0 and the resulting output coordinate files were modified to make them compatible with GROMACS. The resulting structures were energy-minimized using steepest descents method. This was done to remove strain in the polymer backbone and alleviate high energy close contacts. The resulting periodic systems (as shown in Fig. 1) were the starting configurations for all MD simulations.

2.2. Simulations of glass transition temperature

All MD simulations were done using the GROMACS 3.3 simulation package on a 40-node IBM xSeries Linux Cluster. In the simulations, the leapfrog algorithm was used to integrate Newton's equations of motion with a time step of 2 fs. Periodic boundary conditions were applied and nonbonded force calculations employed a grid system for neighbor searching. In this system, only the atoms in the neighboring grid cells are considered when building a new neighbor list. A twin-range cutoff was used for both Lennard-Jones and Coulombic calculations. A cutoff radius of 1.0 nm was used for short-range forces, which were calculated at every simulation step, and a cutoff radius of 1.0 nm was employed for long-range forces, which were calculated during neighbor list generation. In each simulation, the temperature was controlled by employing a Nose–Hoover extended ensemble and the pressure was controlled by employing a Parrinello–Rahman ensemble. Initial velocities were randomly assigned from

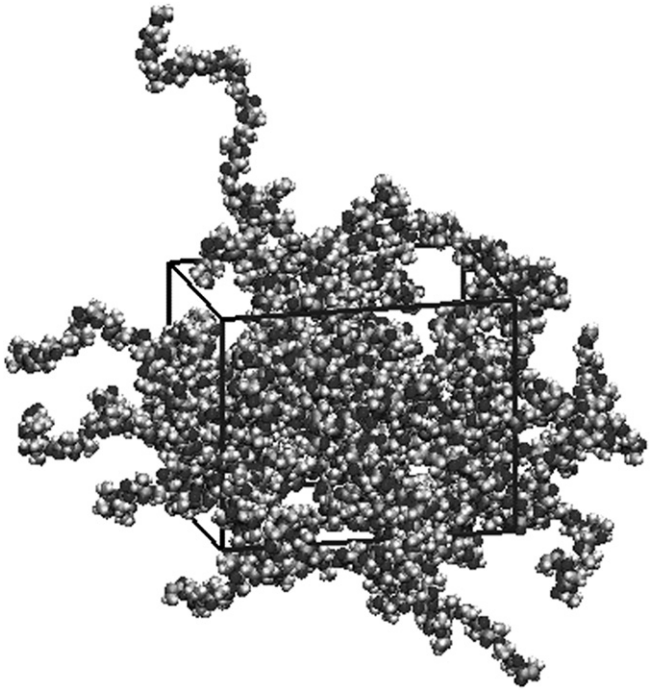

Fig. 1. Snapshot of PLA box starting configuration.

a Maxwell distribution at the selected simulation temperature. The LINCS algorithm was used to constrain all bonds.

For the determination of T_g for a certain molecular weight (polymerization degree $N = 10$, 20 or 30), different simulation boxes (32 PLA chains) are generated, minimized and the lowest energy configuration is chosen. This configuration is further relaxed for 10 ns under NPT conditions 550 K, 1 bar to obtain a well relaxed start structure with the correct density. The specific volume in turn can be readily calculated as the reciprocal of the density. Afterwards, a cooling process is initiated by lowering the temperature stepwise by 50 K until a temperature 200 K is reached. At each temperature 2 ns NPT ensemble dynamics is carried out and the final configuration of this run is used as the starting structure for dynamics at the next (50 K lower) temperature.

3. Results and discussion

3.1. Glass transition temperature

The procedure to determine the glass transition temperature T_g is demonstrated in Figs. 2–4 showing the computed specific volume v as a function of temperature T. The v values are well equilibrated for each temperature within the chosen simulation period (2 ns). Plotted values are mean values of v averaged over the last 1 ns of data sampling at each temperature taking a snapshot every 5 ps. The increase of v with increasing T is less pronounced below T_g yielding a kink in the v versus T curve with the position of it determining T_g. A first rough estimate of the kink position is obtained by visual inspection of the data points. Then, these points are divided into two parts corresponding to the region below (glassy 200 K, 250 K and 300 K) and above (rubbery 400 K and 450 K) this estimate and each set of data is fitted to a straight line by linear regression. The final value of T_g results from the intersection of these two lines.

In Fig. 5 the glass transition temperature versus reciprocal of degree of polymerization plot of three systems with different degree of polymerization N ($N = 10$, 20 and 30) is given. In 1950, Fox and Flory found that the main effect of varying N is a shift of the glass transition temperature (Eq. (2)), where $T_g(\infty)$ is glass transition temperature for infinity molecular weight and C is a constant [45]. The glass transition temperature data were fitted to Eq. (2) by linear regression and R value of the regression is larger than 0.99.

$$T_g(N) = T_g(\infty) - \frac{C}{N} \tag{2}$$

where $T_g(\infty) = 408$ K; $C = 473$.

3.2. Fractal dimension

The radius of gyration is a common size parameter, which describes the size of a polymer chain.

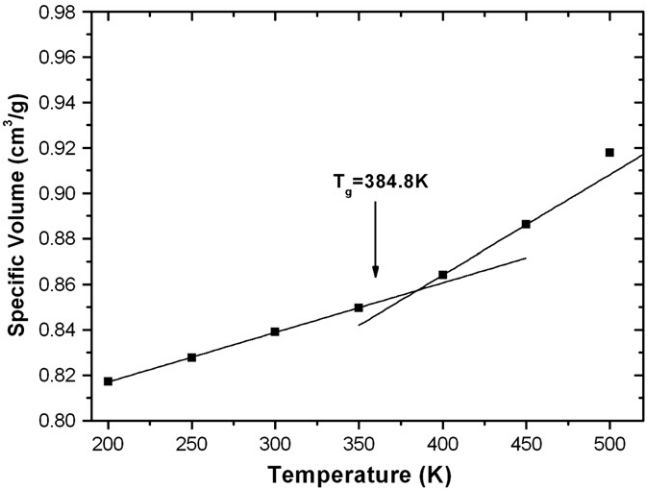

Fig. 3. The computed specific volume v as a function of temperature T for $N = 20$.

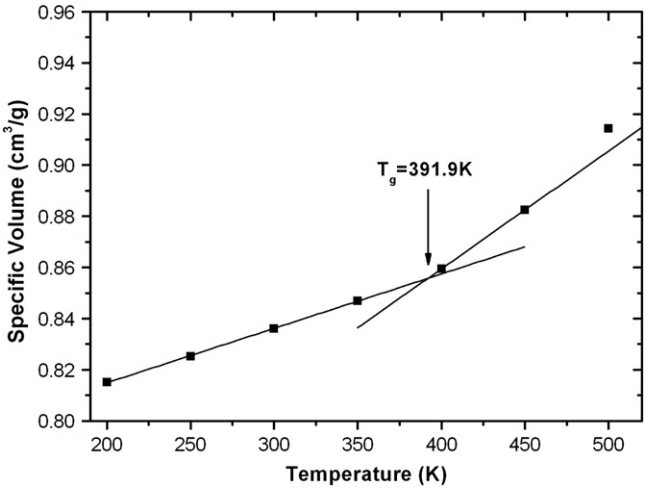

Fig. 2. The computed specific volume v as a function of temperature T for $N = 30$.

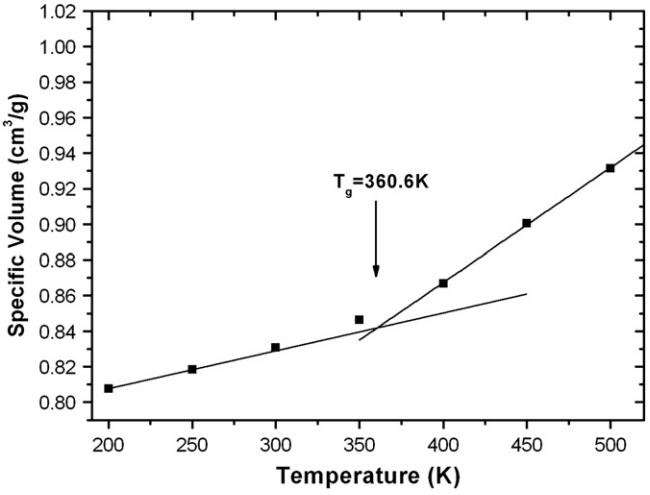

Fig. 4. The computed specific volume v as a function of temperature T for $N = 10$.

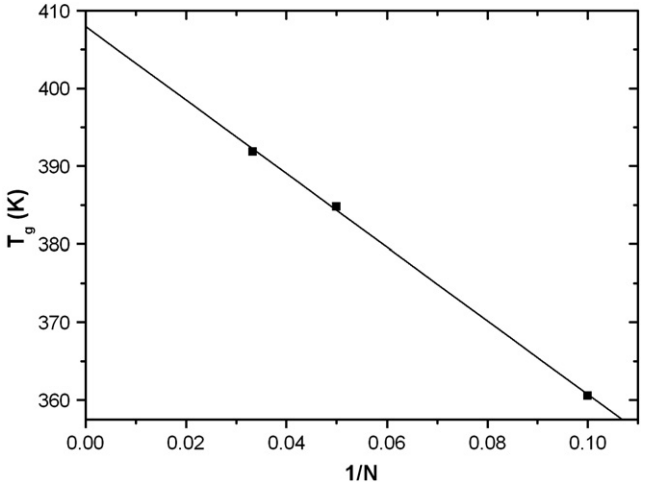

Fig. 5. The glass transition temperature versus reciprocal N plots of three systems ($N = 10$, 20 and 30).

$$R_g = \sqrt{\frac{\sum_i \|r_i\|^2 m_i}{\sum_i m_i}} \tag{3}$$

where m_i is the mass of atom i and r_i the position of atom i with respect to the center of mass of the molecule. Polymers are random fractals, quite different from Koch curves and Sierpinski gaskets, which are examples of regular fractals. The fractal dimension D of any polymer is defined through the relation between the number of monomers N and radius of gyration R_g for a specific polymer, because the root-mean-square size $\sqrt{\langle r^2 \rangle}$ is proportional to the radius of gyration R_g. The typical fractal dimensions are: linear ideal chain $D = 2$, linear chain with short-range repulsion $D = 1.7$ and rigid rod chain is $D = 1$ [46].

$$N \sim \sqrt{\langle r^2 \rangle}^D \sim \left(R_g\right)^D \tag{4}$$

Radii of gyration are calculated at each temperature (Fig. 6) and the R_g increased when the system was cooled but remained constant when the temperature is below glass transition temperature. The $\ln(N)$ and $\ln(R_g)$ values were fitted to a straight line by linear regression (Fig. 7) and the fractal dimension $D = 1.62$.

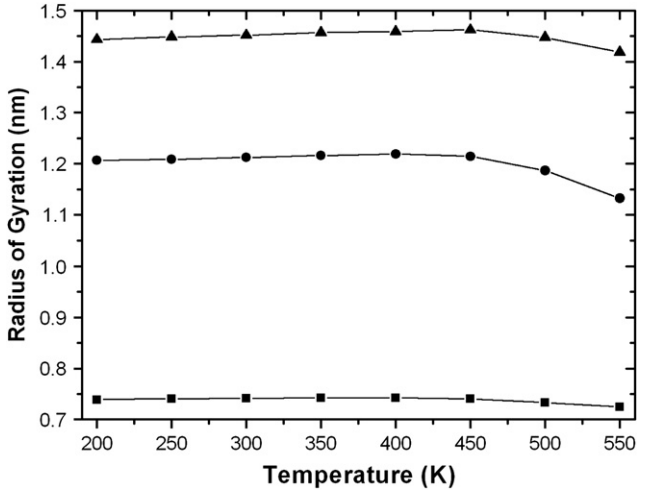

Fig. 6. Radiuses of gyration versus temperature for PLA with different N.

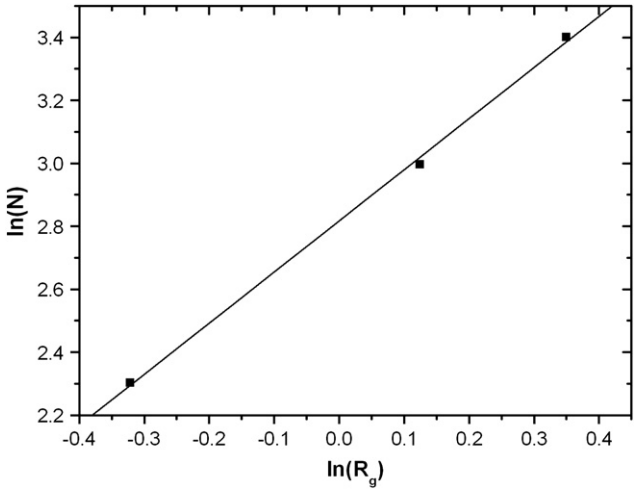

Fig. 7. $\ln(N)$ versus $\ln(R_g)$ for PLA with fractal dimension $D = 1.62$.

3.3. Self-diffusion coefficient

To determine the self-diffusion coefficient D one can use the Einstein relation (Eq. (5)) [47].

$$\lim_{t \to \infty} \left\langle \|r_i(t) - r_i(0)\|^2 \right\rangle_{t \in N} = 6 D_N t \tag{5}$$

The terms in the angular bracket represent the time averaged mean-square displacement (MSD). After approximately 100 ps, the molecules will be moving in a totally random fashion (Brownian motion), and the mean-square deviation of the system will increase linearly as the atoms drift away from each other. The MSD from 200 ps to 800 ps was fitted to a linear curve and the slope is directly related to the self-diffusion coefficient.

The plot of self-diffusion constant D_N versus temperature for PLA with different degree of polymerization (from top to bottom $N = 10$, 20 and 30) is shown in Fig. 8. The

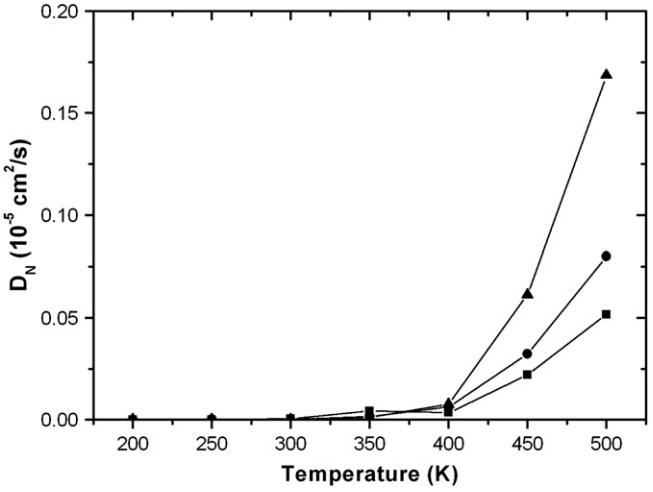

Fig. 8. Plot of self-diffusion constant D_N versus temperature for PLA with different degree of polymerization (from top to bottom $N = 10$, 20 and 30).

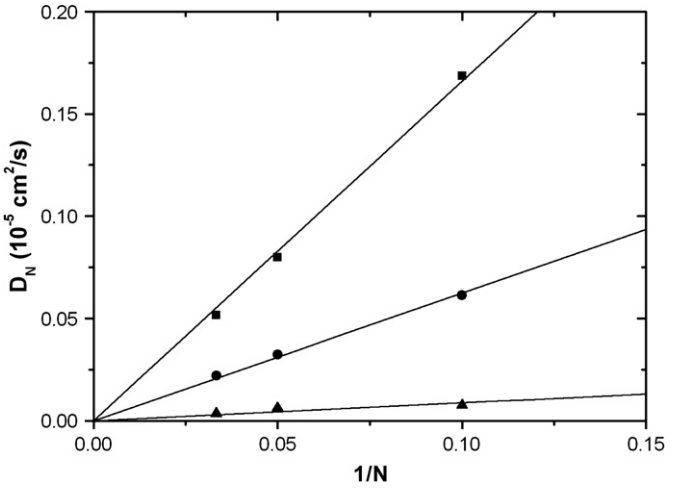

Fig. 9. Plot of self-diffusion constant D_N versus reciprocal of different degree of polymerization $1/N$ (from top to bottom $T = 500$ K, 450 K and 400 K).

self-diffusion constant D_N increased dramatically when the temperature is across glass transition temperature. The plot of self-diffusion constant D_N versus reciprocal of different degree of polymerization $1/N$ (from top to bottom $T = 500$ K, 450 K and 400 K) is shown in Fig. 9. The result agrees with the existing Rouse model that the self-diffusion constant of the chains scales inversely with chain length (Eq. (6)) [46,48].

$$D_N = k_B T/(N\zeta(T)) \tag{6}$$

where $\zeta(T)$ is the friction coefficient experienced by the beads of the chain in their Brownian motion, k_B the Boltzmann's constant, and T is the temperature.

3.4. Shear viscosity

The Rouse model for an unentangled polymer melts shows that the melt viscosity is proportional to the chain length, c being the number of monomers per volume and b being the effective bond length [46,49].

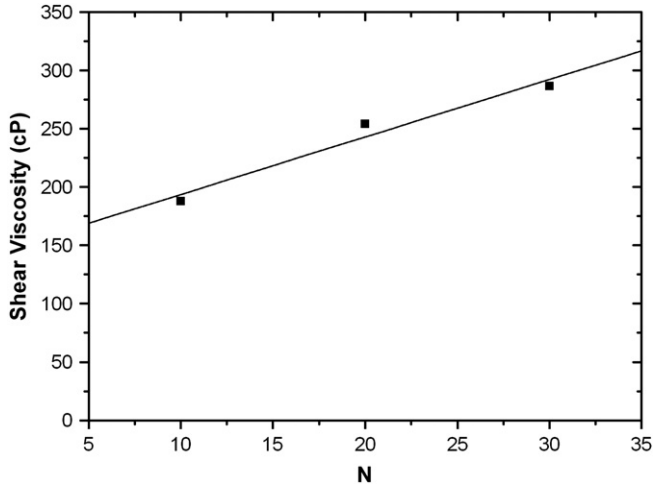

Fig. 10. Plot of shear viscosity versus different degree of polymerization for PLA at 500 K.

$$\eta = c\zeta(T)b^2N/36 \tag{7}$$

The viscosity can be calculated from an equilibrium simulation using an Einstein relation:

$$\eta = \frac{1}{2}\frac{V}{k_BT}\lim_{t\to\infty}\frac{\mathrm{d}}{\mathrm{d}t}\left\langle\left(\int_{t_0}^{t_0+t} P_{xz}(t')\mathrm{d}t'\right)\right\rangle_{t_0} \tag{8}$$

The shear viscosity converged when the temperature is above 500 K. And the plot of shear viscosity versus different degree of polymerization for PLA is shown in Fig. 10. The good agreement between the simulation results and the Rouse model was obtained.

4. Conclusion

Molecular dynamics simulation has been used to investigate the molecular weight dependence of glass transition temperature for amorphous poly(L-lactide). The new PLA force field developed by O'Brien [30] was feasible for the amorphous PLLA systems. The increase of v with increasing T is less pronounced below T_g yielding a kink in the V versus T curve with the position of it determining T_g. The fractal dimension of the PLA systems was 1.62. The self-diffusion constant D_N increased dramatically when the temperature is across glass transition temperature. The molecular weight dependence of glass transition temperature, self-diffusion coefficient and shear viscosity were studied and the good agreement between the simulation results and the Rouse model was obtained.

Acknowledgements

This work was funded by USDA Award No. 2003-38820-14102 awarded to Dr. Lou and DOE Grant DE-FG26-06NT42742 awarded to Dr. Lou. One of the authors, Prof. Jizhong Yan was partially funded by the Visiting Scholarship from China.

References

[1] Richard AG, Bhanu K. Science 2002;297:803.
[2] Drumright RE, Gruber PR, Henton DE. Advanced Materials 2000;12:1841.
[3] Uhrich KE, Cannizzaro SM, Langer RS, Shakesheff KM. Chemical Reviews 1999;99(11):3181–98.
[4] Lee SH, Zhang ZP, Feng SS. Biomaterials 2007;28(11):2041–50.
[5] Zhang ZP, Lee SH, Feng SS. Biomaterials 2007;28(10):1889–99.
[6] Costantino L, Gandolfi F, Bossy-Nobs L, Tosi G, Gurny R, Rivasi F, et al. Biomaterials 2006;27(26):4635–45.
[7] Gomez-Lopera SA, Arias JL, Gallardo V, Delgado AV. Langmuir 2006;22(6):2816–21.
[8] Shi ZQ, Zhou YF, Yan D. Polymer 2006;47(24):8073–9.
[9] Li YY, Cunin F, Link JR, Gao T, Betts RE, Reiver SH, et al. Science 2003;299(5615):2045–7.
[10] Antonov EN, Bagratashvili VN, Whitaker MJ, Barry JJA, Shakesheff KM, Konovalov AN, et al. Advanced Materials 2005;17(3):327–30.
[11] Salem AK, Rose FRAJ, Oreffo ROC, Yang X, Davies MC, Mitchell JR, et al. Advanced Materials 2003;15(3):210–3.

[12] Chen R, Curran SJ, Curran JM, Hunt JA. Biomaterials 2006;27(25):4453–60.
[13] Hurtado A, Moon LDF, Maquet V, Blits B, Jerome R, Oudega M. Biomaterials 2006;27(3):430–42.
[14] Wang L, Jia X, Yuan Z. Polymer 2006;47(20):6978–85.
[15] Ouchi T, Ichimura S, Ohya Y. Polymer 2006;47(1):429–34.
[16] Csihony S, Culkin DA, Sentman AC, Dove AP, Waymouth RM, Hedrick JL. Journal of the American Chemical Society 2005;127(25):9079–84.
[17] Mosnacek J, Duda A, Libiszowski J, Penczek S. Macromolecules 2005;38(6):2027–9.
[18] Majerska K, Duda A. Journal of the American Chemical Society 2004;126(4):1026–7.
[19] Nomura N, Ishii R, Akakura M, Aoi K. Journal of the American Chemical Society 2002;124(21):5938–9.
[20] Ovitt TM, Coates GW. Journal of the American Chemical Society 2002;124(7):1316–26.
[21] Sun L, Ginorio JE, Zhu L, Sics I, Rong L, Hsiao BS. Macromolecules 2006;39(24):8203–6.
[22] Lee WK, Iwata T, Gardella JAJ. Langmuir 2005;21(24):11180–4.
[23] Wang Y, Pfeffer R, Dave R, Enick R. AIChE Journal 2005;51(2):440–55.
[24] Rohman G, Grande D, Laupretre F, Boileau S, Guerin P. Macromolecules 2005;38(17):7274–85.
[25] Tretinnikov ON, Kato K, Iwata H. Langmuir 2004;20(16):6748–53.
[26] Rzayev J, Hillmyer MA. Journal of the American Chemical Society 2005;127(38):13373–9.
[27] Karl GW, Martin M, Andreas K, Gerhard Z. Chemical Physics Letters 2005;406:90–4.
[28] David K, Yiqi Y. Polymer 2006;47:4845–50.
[29] Sheetal SJ, Tejraj MA. Polymer 2006;47:8061–71.
[30] O'Brien CP. Quantum and molecular modeling of polylactide, Ph.D. dissertation, Clemson University; 2005.
[31] Berendsen HJC, van der Spoel D, van Drunen R. Computer Physics Communication 1995;91:43–56.
[32] Binder K, Baschnagel J, Paula W. Progress in Polymer Science 2003;28:115–72.
[33] Paul W, Smith GD. Reports on Progress in Physics 2004;67:1117–85.
[34] Gee RH, Lacevic N, Fried LE. Nature Materials 2006;5:39–43.
[35] Wang XY, Raharjo RD, Lee HJ, Lu Y, Freeman BD, Sanchez IC. Journal of Physical Chemistry B 2006;110:12666–72.
[36] Wang XY, Willmore FT, Raharjo RD, Wang X, Freeman BD, Hill AJ, et al. Journal of Physical Chemistry B 2006;110:16685–93.
[37] Richardson DG, Abrams CF. Macromolecules 2006;39:2330–9.
[38] Makrodimitri ZA, Raptis VE, Economou IG. Journal of Physical Chemistry B 2006;110(32):16047–58.
[39] Momany FA, Willett JL. Biopolymers 2002;63(2):99–110.
[40] Fried JR, Ren P. Computational and Theoretical Polymer Science 1999;9(2):111–6.
[41] Yu KQ, Li ZS, Sun JZ. Macromolecular Theory and Simulations 2001;10:624–33.
[42] Lindahl E, Hess B, van der Spoel D. Journal of Molecular Modeling 2001;7:306–17.
[43] Van der Spoel D, Lindahl E, Hess B, van Buuren AR, Apol E, Meulenhoff PJ, et al. Gromacs user manual version 3.3, www.gromacs.org; 2005.
[44] Jorgensen WL, Tirado-Rives J. Journal of the American Chemical Society 1988;110:1657–66.
[45] Fox TG, Flory PJ. Journal of Applied Physics 1950;21:581–91.
[46] Rubinstein M, Colby RH. Polymer physics. Oxford: Oxford University Press; 2003 [chapter 1].
[47] Allen MP, Tildesley DJ. Computer simulations of liquids. Oxford: Oxford Science Publications; 1987.
[48] Doi M, Edwards SF. The theory of polymer dynamics. Oxford: Clarendon Press; 1986.
[49] Ewen B, Richter DN. Advances in Polymer Science 1997;134:1–129.